

General concepts, assumptions, drawbacks and misuses in Kinetic Monte Carlo and microkinetic modelling simulations applied to computational heterogeneous catalysis

Hèctor Prats, Francesc Illas*, Ramón Sayós*

Departament de Ciència de Materials i Química Física & Institut de Química Teòrica i Computacional (IQTCUB), Universitat de Barcelona, C. Martí i Franquès 1, 08028 Barcelona, Spain.

** authors for correspondence: Francesc Illas and Ramón Sayós
e-mail: francesc.illas@ub.edu, r.sayos@ub.edu*

Abstract

In the present paper, we survey two common approaches widely used to study the kinetics of heterogeneous catalytic reactions. These are kinetic Monte Carlo simulations and microkinetic modelling. We discuss typical assumptions, advantages, drawbacks and differences of these two methodologies. We also illustrate some wrong concepts and inaccurate procedures used too often in this kind of kinetics studies. Thus, several issues as for instance minimum energy diagrams, diffusion processes, lateral interactions or the accuracy of the reaction rates are discussed. Some own examples mainly based on water gas shift reaction over Cu(111) and Cu(321) surfaces are chosen to explain the different developed topics on the kinetics of heterogeneous catalytic reactions.

KEYWORDS

Kinetic Monte Carlo and microkinetic modelling, reaction rates, energy and free energy diagrams, computational heterogeneous catalysis

1. Introduction

Heterogeneous catalysis employing solid surfaces as catalysts for gas reactions has huge impact and many applications in metallurgical and chemical industries. More than 90% of the chemical and energy industries utilize this type of catalysts. In the past two decades, the study of the molecular mechanism of heterogeneous catalysis has led to significant advances and established a systematic approach to obtain total and free energy profiles as well as quite accurate reaction rates derived from transition state theory.^[1,3] The understanding of the kinetics of heterogeneous catalytic reactions experienced similar progress but the available approaches are far from being generally applicable. Clearly, a better understanding of kinetic aspects can help to improve the design of reactors operating in steady-state regime, proposing more suitable initial conditions (i.e., T, P and initial gas composition) or improved catalysts (e.g., with high conversion at low temperatures). Normally, catalytic reactors use porous pellets with nm-sized catalyst particles at the available (external or internal) surfaces of pores. Nowadays, surface science allows one to study the reaction kinetics on catalyst models working on controlled conditions. Similar experiments can be carried out involving surfaces of porous catalysts, pellets and/or the whole reactor, therefore implying different size and time scales.^[2] The present work focuses on those cases, where experimentally single- or poly-crystal samples can be used as catalytic models under ultrahigh vacuum conditions.

Heterogeneous catalytic reactions are complex reactions, which involve frequently a large list of several elementary surface processes, where one or several mechanisms can be competing in both main and side reactions. Usually five consecutive stages are involved: 1) diffusion of reactant species from gas-phase to the surfaces, 2) adsorption of the gases on the surfaces, 3) reaction at the surfaces, 4) desorption of the products, and 5) diffusion of the desorbed products into the gas-phase.^[3] In general, the diffusion processes are faster than the chemical reactions at the surface and the global reaction is not diffusion-limited. The main types of surface processes can be classified as: a) molecular or dissociative adsorptions, b) molecular desorptions, c) unimolecular processes (e.g., molecular dissociation) and d) bimolecular reactions, involving two adsorbed species (i.e., Langmuir-Hinshelwood (LH) step) or involving one gas species and one adsorbed species (i.e., Eley-

Rideal (ER) step) although the later dominates in a limited number of cases. LH and ER reactions can give rise to gas and/or adsorbed products. Moreover, even for pristine well defined single crystal surfaces, several types of sites (e.g., top, bridge, fcc-hollow, hcp-hollow,...), where the same reactants can present different reaction rates (sometimes originating also different products), thus enlarging the already long list of existing elementary surface processes.

Density Functional Theory (DFT) calculations represent a good first-principles approach for a proper description of these individual surface processes, although adsorbate-adsorbate lateral interactions should be included too to account for the significant coverage effects in the reaction kinetics. These DFT data can be used later to study the global catalytic heterogeneous reaction by using mean-field microkinetic modelling (MM)^[3] or kinetic Monte Carlo (kMC)^[4] simulations. Here a caveat is necessary since energy profiles, and hence energy barriers and transition state theory derived reaction rates, are sensitive to the choice of the exchange-correlation method and inclusion of dispersion terms, neglected in many articles in the past, often appears as crucial.

In this paper, we describe in detail how to use both MM and kMC methods to study a heterogeneous (i.e., gas-surface) catalytic reaction, highlighting the main advantages and limitations of these techniques. Moreover, we review and discuss some concepts and inaccurate procedures, used very regularly in this kind of kinetics studies. These mistakes or inaccuracies could be possibly originated from the very multidisciplinary character of this research field, involving scientists from different backgrounds (e.g., chemists, physicists, chemical engineers,...), which is also visible through the wide spectrum of important journals where these studies are frequently published.

2. System model and kinetic methods

A consistent MM or kMC kinetics study on a complex heterogeneously (gas-surface) catalysed reaction should define clearly the model system (i.e., reactor) aimed at closely simulating an experimental kinetic study. This model system involves the choice of a gas model, a lattice model and a reaction model. The gas model normally implies a gas mixture of reactants (sometimes including also inert or product species) at a fixed temperature, total pressure and initial gas composition (i.e., partial pressures). The surface of a real solid catalyst (i.e., exposed surface) can be sometimes modelled by choosing a

given well defined single crystal surface represented by a slab model described by a periodic 2D unit cell (i.e., lattice), and exhibiting one or several types of sites. Finally, the reaction model should include all possible elementary surface processes that are likely to occur in all accessible reaction mechanisms at the selected experimental conditions. Moreover, some extra points should be taken into account if a correct comparison between experiment and simulations is intended. For instance, in a closed reactor the composition of the reactants mixture would change through the reaction. In the case of a plug flow reactor, the total flow rate should also be included into the simulation. Moreover, depending on the type of reactor, the reverse reaction of elementary surface processes producing the final products of the whole reaction should be taken into account, as these product species could react backward (even more if they appear in the initial reactant mixture). Usually, many MM or kMC studies assume an ideal experimental set-up with a fresh reactants mixture continuously impinging on an empty (or gas precovered) thermalized catalyst surface, where the heterogeneous complex reaction takes place and, afterwards, the final gas products desorb and leave the surface region implying a process not in a thermodynamic equilibrium but rather in a steady-state).

2.1 Kinetic Monte Carlo simulations

As surface processes are rare events, direct Molecular Dynamics simulations would require very long run times and are thus computationally prohibitive. This is further complicated by difficulty in defining accurate force fields describing together all surface processes. In principle, one could use ab initio derived forces (AIMD) but, again, the long runs needed make the overall approach unaffordable even by relying on the time-saving steps methods as in the Carr-Parrinello MD (CPMD). Another complication comes from the enormous accumulated errors that would appear in the numerical integration of the trajectories. Thus, an alternative approach is needed where the problem can be solved by making use of stochastic techniques based on Monte Carlo like algorithms. This is the idea behind the so called kinetic Monte Carlo (kMC) method^[4, 5] used to solve numerically the master equation (ME) (*Eq. 1*). To make use of this approach one needs to define an appropriate lattice model defining the state of a gas-surface system. This can be described by defining a surface configuration, where both free and occupied sites are assigned (i.e.,

adlayer configurations). Different surface processes (i.e., adsorption, diffusion, reaction and desorption) will modify continuously the surface configurations.

The ME, which can be derived from first principles,^[4] is a lost-gain equation that governs the time evolution of the probability of any α surface configuration (P_α), Eq. 1

$$\frac{dP_\alpha}{dt} = \sum_\beta [W_{\beta\alpha}P_\beta - W_{\alpha\beta}P_\alpha] \quad (1)$$

Here, the sum runs over all surface configurations, P_α (P_β) denotes the probability to find the system in the surface configuration α (β) at time t and $W_{\alpha\beta}$ is the transition probability per unit time to pass from a configuration α to a different β one in such a way that only one surface process is implied. These transition probabilities (units: s^{-1}) are synonymous to reaction rates ($r_{\alpha\beta}$) of the mentioned surface processes. Sometimes they are also called rate constants ($k_{\alpha\beta}$), but they are not necessarily coincident with the same rate constants used in macroscopic rate equations,^[3] which can have different units (e.g., s^{-1} for a unimolecular reaction or molecular desorption, $m^2 \cdot s^{-1}$ for a LH reaction,...). The ME is solved by using several efficient algorithms such as variable step size, random selection, first reaction, rejection-free,^[4] which can be appropriately selected from analysis of their influence in the numerical solution of the ME and should support the principle of detailed balance for each surface process. Thus, the rejection-free algorithm is widely used to solve the ME in kMC simulations and goes as follows.^[4,5]

1. Generate an initial α surface configuration ($t = 0$), make the list of all possible surface processes ($N_{p(\alpha)}$) and define the sites involved for such processes ($N_{s(\alpha)}$).
2. Determine the $r_{\alpha\beta}$ reaction rates of all $N_{p(\alpha)}$ surface processes from this α surface configuration (i.e., all $\alpha \rightarrow \beta$ processes) and the total reaction rate $r_{tot(\alpha)}$:

$$r_{tot(\alpha)} = \sum_\beta^{N_{p(\alpha)}} r_{\alpha\beta} \quad (2)$$

3. Then, select the surface process $\alpha \rightarrow \alpha'$ that fulfils the following condition,

$$\sum_{\beta < \alpha' - 1} r_{\alpha\beta} < \rho_1 \cdot r_{tot(\alpha)} \leq \sum_{\beta < \alpha'} r_{\alpha\beta} \quad (3)$$

where ρ_1 is a random number generated from a uniform distribution on the unit interval ($\rho_1 \in [0,1]$) and both summations represent the cumulative distribution functions of the reaction rates ($r_{\alpha\beta}$ is the discrete random variable), being their values for surface processes $\alpha \rightarrow \alpha'-1$ ($R_{\alpha,\alpha'-1}$) and $\alpha \rightarrow \alpha'$ ($R_{\alpha,\alpha'}$), respectively.

4. Advance the time, using a second random number

$$t \rightarrow t - \frac{\ln(\rho_2)}{r_{\text{tot}}(\alpha)} \quad (4)$$

5. Update the system to the new surface configuration α' (i.e., adding, moving or removing adsorbed species on the lattice), make the new list of all possible surface processes ($N_p(\alpha')$) and repeat again the cycle from step 2).

Typically, every kMC simulation will involve a huge number of steps (i.e., $10^8 - 10^{11}$) until the system achieves a steady-state (i.e., temporal convergence of coverages (θ) and turnover frequencies (TOF), sometimes also called turnover rates (TOR)). Temporal acceleration of kMC simulations to overcome the problem of the large differences in the time scales of surface processes can be carried out by using more refined algorithms.^[6-8] Additional simple techniques can also be considered to reduce the kMC computational cost, as for instance, the use of scaling factors in reaction rates for the very fast processes (e.g., diffusion rates^[9,10]) or beginning the kMC simulation from a lattice with an initial coverage obtained from a MM solution.

The reaction rates of the different surface processes ($r_{\alpha\beta}$), which are defined as the number of times a process occurs per site and time unit, can be computed by means of collision theory (CT) and/or the transition state theory (TST).^[3,4] For LH reactive processes, desorption processes and atomic or molecular diffusion processes the reaction rates can be calculated by using the canonical TST formula

$$r = \frac{k_B \cdot T}{h} \frac{Q^\ddagger}{Q^R} e^{-\frac{\Delta V^{0\ddagger}}{k_B \cdot T}} \quad (5)$$

where h denotes Planck's constant, k_B the Boltzmann's constant, and Q^\ddagger and Q^R are the partition functions (dimensionless) of the transition state (TS) and the reactants, respectively, which are calculated from standard statistical mechanical expressions.^[11]

$\Delta V^{0\neq}$ represents the energy barrier of the surface process, including the zero-point energy (ZPE) correction. In some works, the term of activation energy (E_a) is inadequately used for labelling ΔV^{\neq} or $\Delta V^{0\neq}$ values. This term should be kept for one of the parameters derived from the empirical Arrhenius equation (the other is the pre-exponential factor, A), which explain the temperature dependence of many reaction rates.^[3]

The rate of adsorption (non-dissociative) processes can be estimated by using the Hertz-Knudsen equation, Eq. 6

$$r_{\text{ad}} = S_0(T) \cdot A_{\text{site}} \cdot \frac{P}{\sqrt{2\pi m k_B T}} \quad (6)$$

where S_0 is the initial sticking coefficient, A_{site} corresponds to the area of a single site, P is the gas partial pressure and m is the molecular mass of the gas species.

The rate of desorption processes, where $\Delta V^{0\neq} = \Delta V_R^0$ (the reaction endothermicity or adsorption energy) can be determined from TST, assuming an early 2D gas-like TS, Eq. 7 and 8,

$$r_{\text{des}} = \frac{k_B \cdot T}{h} \frac{Q_{\text{vib}}^{\text{gas}} \cdot Q_{\text{rot}}^{\text{gas}} \cdot Q_{\text{tras,2D}}^{\text{gas}}}{Q_{\text{vib}}^{\text{R}}} e^{-\frac{\Delta V^{0\neq}}{k_B \cdot T}} \quad (7)$$

$$Q_{\text{tras,2D}}^{\text{gas}} = A_{\text{site}} \cdot \frac{2\pi m k_B T}{h^2} \quad (8)$$

The energy barriers and the vibrational frequencies of minima and transition states are normally calculated from first-principles by using DFT calculations^[1,12] although the choice of the DFT method requires some caution and, whenever possible, calibration by comparison to available accurate experimental data. Moreover, additional DFT calculations are necessary to introduce also the adsorbate-adsorbate lateral interactions for all reactant and product pairs (*vide infra*), which may affect the values of the energy barriers of the surface processes (i.e., coverage-dependent energy barriers) and hence their reaction rates, becoming especially important for high coverage situations.

Note also that kMC method applied to the study of heterogeneously catalysed gas-phase reactions is not limited only to flat crystal surfaces; it can also be used for simulating

complex systems such as surface reactions on supported nanoparticles exhibiting different facets.^[13]

2.2 Microkinetic modelling

Kinetic models can be used for the study of many complex reactions (e.g., gas-phase, solution-phase or gas-surface processes), including also the transport phenomena when they are relevant (i.e., diffusivity, viscosity and heat conduction). These models afford treating several kinds of experimental reactor models.^[14] When dealing with the reaction kinetics on pore or crystalline solid surfaces, simpler microkinetic models can be used in a similar way as it was explained before for kMC simulations.^[15, 16] In this case, macroscopic rate equations (*Eq. 9*) are applied to describe all surface processes involved in the proposed reaction model, usually within the mean-field approximation, in which it is assumed that the adsorbates are uncorrelated,

$$\left(\frac{d\theta_i}{dt} = \sum_j v_{ij} r_j f_j(\theta_1, \dots, \theta_N) \right)_{i=1,N} \quad (9)$$

where θ_i is the surface coverage of i species at time t (among the all N possible adsorbates), v_{ij} is the stoichiometric number for i species in j surface process (positive or negative for species formation or removal, respectively), r_j the reaction rate and f_j is a function of several coverages involved in the j surface process; the summation covers all possible surface processes where the i species is involved. Frequently, these equations are expressed using rate constants (k_j), which are easily related with reaction rates (r_j). DFT data along with TST and CT can be applied to determine the reaction rates from first-principles as already explained for kMC simulations. However, sometimes they can be used as fitting parameters together with some available values of experimental rate constants aiming to reproduce the observed experimental global reaction kinetics data, assuming a reasonable reaction mechanism. Clearly, such empirical fitting hinders a validation of the proposed mechanism.

The set of coupled differential equations are numerically integrated until steady-state values of coverages and TOFs are achieved. Apparent activation energies (E_a^{ap}) and partial reaction orders (α_i) can also be derived from the values of total reaction rates by

using either the net overall reaction rate r_{net} (the forward minus the reverse reaction rate) or the forward reaction rate r_f ,

$$E_a^{\text{ap}} = k_b T^2 \cdot \left(\frac{\partial \ln(r_f)}{\partial T} \right)_p \quad (10)$$

$$\alpha_i = \left(\frac{\partial \ln(r_f)}{\partial \ln[i]} \right)_p \quad (11)$$

that also can be calculated in kMC simulations in a similar way, and compared later with experimental values.

2.3 kMC vs. MM studies

The simplest possible comparison between kMC and MM methods for a given complex gas-surface reaction involves assuming the same gas model, lattice model and reaction model (i.e., the same number of surface processes including also diffusion). kMC gives a stochastic solution of the ME whereas MM provides a deterministic solution of the differential rate equations (*Eq. 9*). However, a first difference arises from the assumption of uniform coverages in mean-field MM, while kMC simulations reveal the existence of structures or ordered adlayers even at high temperatures. Moreover, kMC and MM predicted TOFs and final average coverages are usually different.^[4] For instance, compared to similar kMC simulations, mean-field models can overestimate the catalytic activity by several orders of magnitude as shown in the case of CO methanation on stepped transition metal surfaces.^[6] This is the case even when lateral interactions are neglected in both methods.

In general, a considerable number of early published mean-field MM studies disregards lateral interactions,^[17-19,50] which are very important for the overall reaction as kMC studies show. However, MM beyond the mean-field approximation have been successfully applied for methane oxidation over PdO(101), subdividing the relevant adsorbates into “paired” and “unpaired” species,^[16] obtaining a good agreement with a range of experimental findings. To include these lateral interactions, the coverage dependence of the energy barriers of the surface processes is also included in some recent MM studies as in the case of ethylene hydrogenation over transition metal surfaces.^[20]

From a practical point of view, kMC simulations have a larger computational cost than for corresponding MM simulations applied to the study of catalytic heterogeneous reactions based on first-principles DFT data. However, this is a fraction of the computational cost required to obtain the CT and TST rates and, on the other hand, kMC method allows an easier and deeper introduction of complex lattice models including for instance explicit or grouped kinds of sites, mono- or bidentate-adsorbed species, diffusion processes and lateral interactions than using MM methods.

Finally, a direct comparison of kMC and MM simulations about the time evolution of the surface reactions is not appropriate. In spite of using the same reaction rates which in fact represent thermally averaged values, the stochastic kMC time evolution of the rejection-free algorithm is governed by *Eq. 4*. Hence the step-time to advance the clock is independent of the process which is chosen.^[5] For instance, for a selected surface process $\alpha \rightarrow \alpha'$ compare $1/r_{\text{tot}(\alpha)}$ and $1/r_{\alpha \alpha'}$, which are different from the deterministic time propagation followed in MM simulations (*Eq. 9*). Finally, it is worth pointing out that neither kMC nor MM match the real-time evolution of the experimental surface reactions, being the experimental and theoretical comparisons made mainly through the final steady-state properties such as TOFs, coverages, degrees of rate control, among others.

3. Discussion of some topics related with kMC and MM studies

3.1 Water gas shift reaction as an example

In order to illustrate and discuss several topics that appear in both kMC and MM kinetic studies of complex gas-surface reactions, we have selected as an example the water gas shift reaction (WGSR) on the flat Cu(111)^[10] and on the stepped Cu(321)^[21] surfaces, that have recently studied by means of kMC simulations.

Two general reaction mechanisms have been proposed for the WGSR on metal-based catalysts, both starting with water dissociation. Next, in the so called redox mechanism, carbon dioxide is formed by direct reaction between adsorbed CO and O, whereas the so called associative mechanism is based on the formation of a carboxyl intermediate (see Figure 1). The associative mechanism has been found to be the most important in both surfaces and has been selected in the present study for the construction of several minimum energy diagrams and to better explain the issues discussed below.

Nevertheless, all kMC simulations were performed including both mechanisms in the reaction model. A complete list of all surfaces processes can be found in previous works.^[10,21] In the case of the Cu(111) surface, all terrace sites were considered equivalent, and only pairwise additive lateral interactions between neighbouring CO adsorbates were included. Moreover, diffusion processes for the most mobile species (essentially CO, H₂O, OH and O) were added into the reaction model. On the other hand, in the study of the Cu(321) surface, different types of sites were distinguished, and pairwise interactions for all possible reactant and product pairs were included using a cluster expansion model.^[22, 23] Additionally, diffusion processes for H₂O, OH and O species were included as in the case of the Cu(111) surface. All kMC calculations have been carried out by means of ZACROS code,^[22, 24] although some of them used also an in-house developed C++ code.

3.2 Construction and use of several kinds minimum energy diagrams

DFT-based calculations carried out on suitable periodic surfaces, complemented by statistical thermodynamics, is currently the main tool to investigate heterogeneously catalysed reactions at the molecular level.^[1, 12] These constitute a necessary previous stage to kMC or MM studies. This computational framework allowed us to calculate accurate minimum energy diagrams for many complex processes involving several elementary steps with detailed information about transition states and stable intermediate species. From the minimum energy profiles the equivalent pictures for Gibbs free energies can be obtained, which summarize the proposed reaction model or the main reaction mechanisms observed in kMC or MM studies. Nevertheless, the construction, the use and the interpretation of these energy diagrams needs to be handled with caution.

Minimum energy diagrams based on DFT calculated total energies lead to potential energy diagram (PED). These, should include the ZPE correction and provide a first view of a given reaction mechanism. ZPE can be calculated for a harmonic oscillator model as a sum of contribution from all vibrational modes. Low frequencies ($< 500 \text{ cm}^{-1}$) do not contribute to ZPE, while high frequencies can contribute with several tenths of eV.^[1] This trend is opposite to that of the frequency contribution to the entropy, as discussed later. ZPE correction is especially important in surface reactions involving H atoms, like water dissociation or hydrogenation reactions, because the atom-H stretching frequencies are typically between $3000\text{-}4000 \text{ cm}^{-1}$. Figure 2 shows the effect of the inclusion of the ZPE

correction on the PED for the WGS on Cu(321) (associative mechanism). Small differences of up to 0.22 eV can be observed in some energy barriers (i.e., water dissociation), which have large effects on the corresponding reaction rates. For instance, the reaction rate corresponding to the water dissociation at 625 K including ZPE is $1.5 \cdot 10^6 \text{ s}^{-1}$, whereas the value without ZPE is only $2.5 \cdot 10^4 \text{ s}^{-1}$, 60 times smaller! Therefore, ZPE should always be included in all energy barriers (i.e., $\Delta V^{0\neq}$) used for reaction rate calculations (e.g., in *Eqs. 5 and 7*).

The commonly GGA functionals widely used in past years neglect dispersion terms, which may play an important role in chemical and physical processes. Dispersion interactions largely affect the adsorption properties of molecules at surfaces, and can be the dominant term as in the case of aromatic molecules interacting with the basal plane of MoS₂,^[25] graphene on metallic surfaces^[26] or hydrocarbons interacting with zeolites.^[27] Even if the process being studied involves small size species such as, CO or CO₂ only, the contribution of dispersion interactions to the overall energy may be important and should not be ignored. In a previous study on the effect of vdW interactions in the WGS on Cu(321),^[28] it has been shown that the dispersion contribution is different for reactants, intermediates and products, with a clear net effect and with no compensation of errors. These terms affect adsorption structures and adsorption energies but also the overall PED, producing tremendous changes in the predicted reaction rates. For instance, the calculated binding energy of CO₂ on Cu(321) surface is increased from 0.06 to 0.28 eV when vdW corrections are included (i.e., at PBE-D2 level), resulting in a desorption reaction rate 60 times smaller (at T = 625 K). Another example is the energy barrier associated to the carboxyl disproportionation by hydroxyl (i.e., COOH + OH → CO₂ + H₂O) for the same system, which decreases from 0.55 to 0.33 eV when dispersion forces are included, resulting in an increase of a factor of also 60 in the reaction rate (at T = 625 K). Consequently, dispersion terms should be always included when aiming at obtaining reliable information to be used in MM or kMC approaches. Fortunately, most of the often-used codes include the contribution of dispersion terms even if the choice of the appropriate methods is still a matter of debate.^[29]

PEDs are good tools to have an overview of the different elementary reaction steps in a complex surface reaction such as the WGS. However, for processes involving large

shifts in entropy (e.g., adsorption and desorption), they often fail to make even qualitative predictions. Gibbs free energy diagrams are more useful for making such predictions (e.g., the most favourable mechanisms, accurate reaction rates,..), because they take into account the effects of pressure and temperature. Figure 3 shows the Gibbs free energy diagram for the associative mechanism of the WGS on Cu(321). The process is even exothermic at temperatures as high as 625 K but becomes about thermoneutral at 1000 K and endothermic at even higher temperatures. The PED and the Gibbs free energy diagrams are very different, mainly regarding the adsorption and desorption processes. This is because in for molecules in the gas phase, the largest fraction of the standard entropy contribution arises from the translation degrees of freedom, while the vibrational and rotational parts constitute a minor contribution. For adsorbed species, the translational and rotational degrees of freedom become constrained and turn into vibrational degrees of freedom (i.e., frustrated translational and rotational modes). The Gibbs free energy of adsorption is commonly estimated by an approximate procedure proposed by Nørskov et al.^[1] where, in absence of mechanical work, the enthalpy of adsorption is approximated by the corresponding change in the potential energy, the entropy of gas-phase is computed by taking into account all contributions to the partition function with the assumption of rigid rotor and harmonic frequencies, and finally the entropy of adsorbed species can be neglected or computed from the vibrational modes.

However, as in kMC and MM studies the reaction rates need to be calculated for all surface processes, their values can also be used to determine the standard free energies of activation for each surface process ($\Delta G^{0\ddagger}$), using the thermodynamic formulation of TST expression (Eq. 12),

$$r(T) = \frac{k_B \cdot T}{h} e^{-\frac{\Delta G^{0\ddagger}(T)}{k_B \cdot T}} \quad (12)$$

The standard free energies of reaction for each surface process (ΔG^0) can be obtained by using the rates of forward and reverse processes and the detailed balance principle,^[30] Eq. 13,

$$\frac{r_{\text{forward}}(T)}{r_{\text{reverse}}(T)} = e^{-\frac{\Delta G^0(T)}{k_B \cdot T}} \quad (13)$$

From *Eqs. 5 and 12* one can derive a simple relationship between $\Delta G^{0\ddagger}$ and $\Delta V^{0\ddagger}$, *Eq. 14*,

$$\Delta G^{0\ddagger} = \Delta V^{0\ddagger} - k_B T \ln \left(\frac{Q^\ddagger}{Q_R} \right) \quad (14)$$

The contribution to the partition functions (i.e., Q^\ddagger and Q^R) for a given vibrational mode (q_i) is large for low vibrational frequencies, and viceversa, contrary to what happened with the ZPE correction to the energy barrier. Vibrational frequencies larger than 1000 cm^{-1} have a negligible contribution to the total partition function (i.e., $q_i \approx 1$), while frequencies below 50 cm^{-1} give significant contributions to Q (i.e., $q_i > 10$). In the free energy diagrams shown in many published works, it is commonly assumed that the entropy contributions of adsorbed species are zero,^[31] which means that for a given surface process $Q^\ddagger/Q_R \approx 1$ and hence $\Delta V^{0\ddagger} \approx \Delta G^{0\ddagger}$ as derived from *Eq. 14*. However, this usual assumption may not be valid in surface processes involving more than 4 atoms (with a large number of low vibrational modes) or at high temperatures. In the WGSR example at $T = 625 \text{ K}$, most of the elementary steps satisfy that $|\Delta V^{0\ddagger} - \Delta G^{0\ddagger}| < 0.10 \text{ eV}$, but for certain processes $|\Delta V^{0\ddagger} - \Delta G^{0\ddagger}|$ is very large (e.g., for $\text{CO}_2 + \text{H}_2\text{O} \rightarrow \text{COOH} + \text{OH}$, being $\approx 0.35 \text{ eV}$), as shown in Table 1, and it can no longer be assumed that $\Delta V^\ddagger \approx \Delta G^\ddagger$. This also holds for adsorption and desorption processes.

Another feature observed when looking in detail at minimum energy diagrams is that sometimes the ΔG^0 or ΔV (with ZPE) values reported for the overall reaction are different from the DFT values computed directly from gas-phase species (i.e., using only reactants and products). For instance, in the PED of Figure 3 one can see that for WGSR on Cu(321) the value of ΔV is -0.84 eV whereas a value of -0.80 eV is obtained from DFT gas-phase calculations. The differences in ΔG^0 are even larger (e.g., at 525 K , compare -0.55 eV (Fig. 3) against -0.48 eV (Table 2) at PBE level). For other systems, these differences can reach up to several tenths of eV. Clearly, this comparison between gas phase and through the surface calculated thermodynamic values has to be investigated and for large discrepancies further studies are require finding out their origin and to minimize them. A possible e reason for this disagreement is that adsorbed species may react from several adsorption sites (i.e., top, bridge, hollow,...), and the binding energy at each site is really different. Diffusion processes are often not included in minimum energy diagrams,

leading to an inaccurate value of ΔV for the overall reaction. Another reason is that occasionally these energy diagrams are constructed from energy barriers for coadsorbed reactants and products, instead of using the energy barriers at infinite separation on the slab. Finally, in DFT calculations only the slab and the reactant species for a given step are included, while spectator species are missing. This implies a lack of consistency in the energy calculations simply because the unit cells are different. In the case of using a plane wave basis set this implies a different number of plane waves for the same kinetic energy cut-off whereas in the case of using atomic like basis sets such as Gaussian type orbitals or numerical orbitals one faces the problem of basis set superposition error. Ideally, a much more accurate calculation including all possible reaction intermediates is possible but this would require the use of very large supercells, with a concomitant unaffordable increase in the computational cost.

Finally, it is worth pointing out that a comparison between theoretical and available experimental ΔG^0 values, specially for the overall reaction, can and should be done to check even more the quality of the DFT data, which may slightly affect the PED but largely affect the final kMC or MM results. Most often, commonly used GGA type functionals are accurate enough to provide physically meaningful results. Table 2 compares the experimental values of the equilibrium constants (K_{eq}) and ΔG^0 ^[32] for the WGSr at two temperatures (525 and 625 K) with some calculations carried out by means of GAUSSIAN code^[33], using different quantum chemistry methods. Despite being the most used functionals for metallic systems, both PW91 and PBE poorly describes the thermochemistry of WGSr, although the agreement with experiment is better at higher temperature. Even the broadly used B3LYP functional, which was designed precisely to improve the thermochemistry of gas-phase molecules^[34,35] reports an equilibrium constant which is around 45 times larger than the experimental value at 625 K. Only the golden standard CCSD(T) method exhibits a pretty good agreement, though not perfect, with experiment.

At this point, one may argue that results obtained from DFT calculations of reactions taking place at metallic surfaces are doubtful. However, this claim is incorrect because, unlike for gas-phase chemistry, when a reaction takes place above a metallic surface the electrons in the reacting species are largely screened by the electrons in the

conduction band and, in addition, constitute a fraction of the total number of electrons. This is an important remark since it is well-established that both PBE and PW91 GGA type functionals provide a very good description of the metal properties,^[36,36-38] while hybrid functionals, describing better the thermochemistry in gas-phase, fail^[39,40] because of the failure to attain the exact homogeneous electron gas limit.^[41] The large body of literature showing good agreement between DFT calculations at the GGA level with experimental values for adsorption and reaction energies^[20,21] supports this view, and it is reinforced by the evidence that the transition states for reactions catalysed by non-magnetic metals do not evidence any spin polarization.^[42] Moreover, note that most of the available kMC studies correspond to open systems in a nonequilibrium state. Thus, even if the calculated results for reaction rates and related properties are by no means exact, it is very likely that the overall physical description is correct.

3.3 Modelling fast processes

A diffusion (usually fast) process can be represented as a hopping of an adsorbate from one site to a neighbouring one on the lattice model. Although sometimes ignored,^[43] it is important to include diffusion steps of the mobile species into the reaction model since diffusion controlled processes cannot be discarded beforehand. When various site types are distinguished in the lattice model, ignoring diffusion processes can have as a consequence that important intermediate species are not formed during the simulation. For instance, in the kMC model of the WGS on the stepped Cu(321) surface, OH species are produced from water dissociation on bridge sites, but they must migrate to hollow sites to react with CO species in order to produce the COOH species. On the other hand, in the kMC study of the WGS on the flat Cu(111) surface, all adsorption sites were considered equivalent (i.e., all sites are labelled as terrace sites). However, in spite of product molecules can be formed without including diffusion in the reaction model for this simple lattice model, calculated values of TOFs and coverages (Table 3) are different enough from the values obtained when including diffusion processes.

The vast majority of complex heterogeneous reactions contain processes with very dissimilar reaction rates. The slowest surface processes are commonly chemical reaction processes with high energy barriers of up to 2 eV. On the other hand, the fastest ones are usually diffusion processes with energy barriers of only a few hundredths of eV and quite

often adsorption/desorption processes can be also very fast. At a temperature of 625 K a slow surface process with an energy barrier of 1.6 eV will have a reaction rate of around 1 s^{-1} , while the reaction rate for a fast diffusion process with an energy barrier of only 0.05 eV will be around 10^{12} s^{-1} , implying that along the kMC simulation the diffusion will dominate and extremely long simulation are required to observe some evolution of the overall chemical process. Some solutions to improve the performance of kMC simulations were mentioned in section 2.1. For instance, a reduction by some constant factor of the reaction rates of these fast processes has been successfully applied in many kMC studies,^[10,10,21,44] but not all fast processes can be correctly scaled. Another alternative but equivalent solution is to increase all the energy barriers of these processes by the same amount.^[45]

Chatterjee and Voter^[7] developed a temporal acceleration scheme by automatically modifying the reaction rates of fast processes without the need for the user to specify these processes in advance. In this method, called accelerated superbasis kinetic Monte Carlo (AS-kMC), the algorithm keeps track of how often configurations are revisited. When this occurs too often one has an indication of the system being stuck in a set of configurations connected by fast processes (i.e., the superbasis). The reaction rates of these processes are then decreased. This procedure may be repeated until the fast processes are slowed down enough so as escape from the superbasis finally occurs. However, the fact that AS-kMC identifies processes based on the configuration of the entire system is likely to makes it not efficient enough for complex reaction models such as, WGSR or Fischer-Tropsch synthesis where an enormous number of possible configurations needs to be considered. This latter problem was addressed in the recently developed algorithm by Dybeck and coworkers,^[8] where the acceleration is accomplished by reducing the reaction rates of the fast-quasi-equilibrated processes to enable more frequent execution of the slower reactive surface processes. The main improvement is that the partitioning and the scaling is applied to all of the processes in a given reaction channel rather than to the individual processes as done in the Voter scheme. This method has been successfully applied to model the Fischer-Tropsch synthesis reaction over ruthenium. However, the procedure may not be optimum since Andersen et al. used this algorithm to model the CO methanation on stepped transition metal surfaces finding poor accuracy in certain situations.^[6]

3.4 Coadsorption and lateral interactions

A physically meaningful representation of the description of the kinetics of complex surface reactions requires a quantitative account of the lateral interactions between coadsorbed species. Figure 4 shows the PED for a bimolecular surface reaction $A + B \rightarrow C + D$ at zero-coverage limit, this is in a situation where only reactants or products and no spectator species are present at the surface. These interactions can be attractive or repulsive for either reactants or products as shown in Figure 4. At low temperature, these interactions can lead to any correlation in the occupation of neighbouring sites or even result in island formation or ordered adlayers. Only at very high temperatures they will become negligible, which is where mean field approximation is valid and MM simulations meaningful.

Lateral interactions in small systems are commonly described with a cluster expansion model [22,23,46]. This expansion can be made so as to reproduce both the energy profile for reactants at infinite separation and for coadsorbed states (Figure 4) for all the elementary steps. Moreover, energy barriers at a given coverage can be parameterized relying on Brønsted–Evans–Polanyi (BEP) relationships.[47,48] As an example, consider the $\text{COOH} \rightarrow \text{CO} + \text{OH}$ step of the WGS on Cu(321).[21] The energy barrier value used for the calculation of the reaction rate is 0.24 eV, without any neighbouring adsorbates (i.e., zero-coverage limit). However, the presence of other adsorbed molecules can increase the value of the energy barrier of this step up to 0.30 eV, depending on the new lateral interactions that could appear if this process was executed in kMC simulations. Table 2 shows the significant effect of the lateral interactions between coadsorbed species in the kMC calculations for the WGS on Cu(321)[21] even at low pressures and high temperature, where these effects should be lesser.

Due to the high number of species and site types present in complex reaction mechanisms (e.g., in WGS), it is impossible to obtain a complete data set of DFT energies for all possible lateral interactions, which could appear through the reaction (i.e., at high coverages). Thus, kMC models for such complex systems typically employ simpler models for the adlayer energetics. One possibility is then to truncate the cluster expansion to one-body terms and pairwise interactions only for all possible reactant and product pairs, as done in Ref. 21. Fortunately, many lateral interactions are small enough and a cheaper, although less accurate, alternative is to use the energy barriers at infinite separation and

to include only the most important lateral interactions between nearest neighbours, assuming that those lateral interactions are pairwise additive; this was the choice in Refs. 9 and 10.

3.5 *Quality of reaction rates*

The accuracy of the reaction rates used in MM and kMC calculations completely determines the quality of the final results of these simulations. Usually rates are obtained from canonical TST and CT. Most likely, variational TST^[3] would be more appropriate, as shown for gas-phase reactions when comparing calculated to experimental data.^[49] However, VTST requires a significantly large set of DFT data including many configurations along the minimum energy path between the TS and reactants and products. Hence, it has seldom used in this kind of studies. Additionally, for surface processes involving light atom/molecule transfers, a one-dimensional tunnelling correction factor in the reaction rates can be introduced, for instance assuming an Eckart barrier.^[10]

As mentioned above, the use of TST implies obtaining the necessary DFT data of the adsorbed reactants and products and TSs which implies not only structural data but energy barrier and vibrational frequencies as well which are needed to apply Eq. 5. Unfortunately, most of the published works describing the main elementary surface processes of a given complex reaction at a DFT level, report the largest vibrational frequencies of the stationary points (i.e., minima and TS) only.^[50, 50-52] Neglecting these frequencies has almost no effect on the PED of the reaction, but it can lead to large errors in the Gibbs free energy diagrams and in the calculation of the reaction rates, as discussed above. Figure 5 shows the effect of neglecting the frequencies below 500 cm⁻¹ on the Gibbs free energy diagram for the WGS on Cu(321). The most drastic changes are found in the adsorption and desorption processes, due to the underestimated value of Q_R , resulting in an erroneously high value of r_{des} .

3.6 *Proposal of plausible mechanisms and catalysts*

Compared to PED profiles, Gibbs free energy diagrams provide a more detailed picture of the overall surface reaction network. Both diagrams should be used to unravel the underlying molecular mechanism although with the necessary caution when aiming to

make predictions regarding the performance of a given catalyst for a given complex gas-surface reaction. Establishing a ranking of plausible reaction mechanisms and the most efficient catalysts based only on the values of energy barriers of some forward processes (e.g., the rate-determining steps (RDSs)) is not always fully justified although this is often the choice in many studies.^[54, 53-55] Very low energy barriers for reverse processes can greatly hinder reactivity, even if the forward energy barrier is affordable. Moreover, the RDSs may change from one catalyst to another, or even simply by changing the temperature or the reactants partial pressures, and these steps may not coincide with the processes having the highest energy barriers in the energy diagrams.^[21] For instance, consider again the WGS on Cu-based catalysts. It is commonly accepted that the initial water dissociation is the RDS on pure metal surfaces.^[Error! Marcador no definido.] The forward energy barrier for this process on the stepped Cu(321) surface is 0.78 eV,^[21] lower than the 1.01 eV energy barrier for the flat Cu(111) surface.^[10] Thus, one may assume that the stepped surface is more efficient than the flat surface. However, the values for the energy barrier of its reverse process are 0.60 eV and 1.15 eV for the stepped and the flat surface, respectively, making the Cu(111) surface more suitable for WGS, as found by computing the H₂ TOF. Moreover, inspection of the RDSs using a combination of kMC simulations and Campbell's degree of rate control^[56, 57] shows that CO₂ formation by carboxyl intermediate is really more limiting than water dissociation in all temperature and pressure range studied for the WGS on Cu(321).^[21]

Therefore, in order to draw any reliable conclusion on the overall complex reaction, apart from the construction and the previous examination of the mentioned minimum energy diagrams, it is also necessary including the contribution of all reverse processes together with the concentrations of all adsorbed species (or their coverages). Thus, kMC or MM methods along with reliable determination of RDSs are the appropriate methods to obtain a detailed information of the time evolution of complex heterogeneously catalysed reactions catalysis.

4. Concluding remarks

In the present work, kinetic Monte Carlo and Microkinetic Modelling methods applied to the study of the heterogeneous catalysis by using first-principles data based mainly on Density Functional Theory are critically reviewed yet details on both methods are given, which also could serve as a short tutorial for beginners in this area. Several important issues that need to be taken into account appear usually in kMC and MM kinetic studies of complex gas-surface reactions are highlighted. To illustrate the discussions, we rely on recent work on the water gas shift reaction on the flat Cu(111) surface and in the stepped Cu(321) surface. Several additional kMC calculations were also carried out to better support our conclusions.

The effect in kMC and MM studies of the inclusion of dispersion energies in the DFT calculations, of the inclusion of diffusion processes into the reaction model or of the addition of adsorbate-adsorbate lateral interactions has been analysed in detail. Moreover, the accuracy of calculated reaction rates, with a noteworthy effect in the final results, is also examined.

A throughout description regarding the construction, use and interpretation of minimum potential energy and minimum Gibbs free energy diagrams is presented. The results of kMC simulations show that extracting reliable conclusions on the overall complex reaction based on these diagrams, specially using PEDs, only may lead to misleading conclusions. A meaningful simulation requires also including the contribution of all reverse processes together with the concentrations of all adsorbed species. Hence, kMC or MM methods should be applied to correctly treat complex reactions with heterogeneous catalysis.

From the overall discussion, it appears that kMC method offers a more detailed picture of the overall process than that arising from MM. In fact, kMC facilitates an easier and deeper introduction of several important features: refined lattice models, diffusion processes and lateral interactions. However, kMC involves higher computational cost and the need to construct appropriate lattice models, which is far from being automatic. Moreover, more efficient kMC algorithms are needed to better account for surfaces processes with very dissimilar reaction rates.

Acknowledgments

Financial support to this research has been provided by the Spanish MINECO CTQ2014-53987-R and CTQ2015-64618-R grants and, in part, from the Generalitat de Catalunya grants 2014SGR97, 2014SGR1582 and XRQTC. HPG thanks Generalitat de Catalunya for a predoctoral FI-DGR-2015 grant and FI acknowledges additional support from the 2015 ICREA Academia Award for Excellence in University Research.

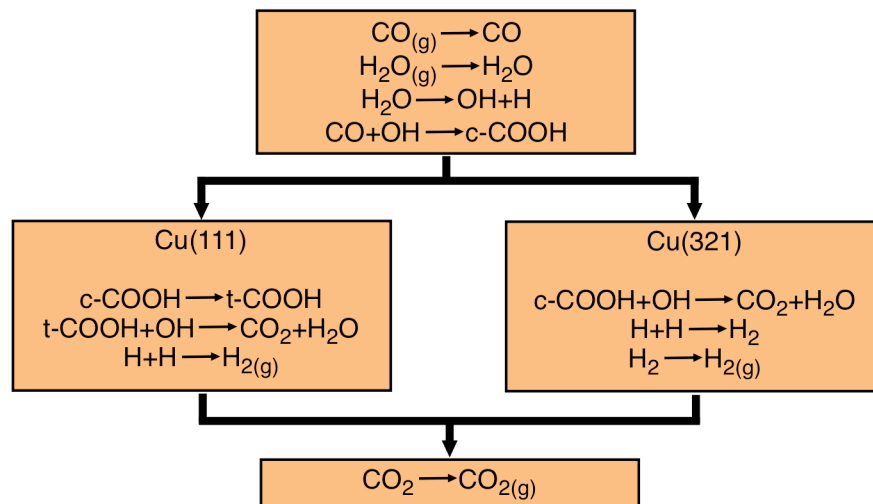


Figure 1. Simplified reaction model of the WGS with an associative mechanism on Cu(111) and Cu(321) surfaces. Note that forward and backward reactions have to be taken into account.

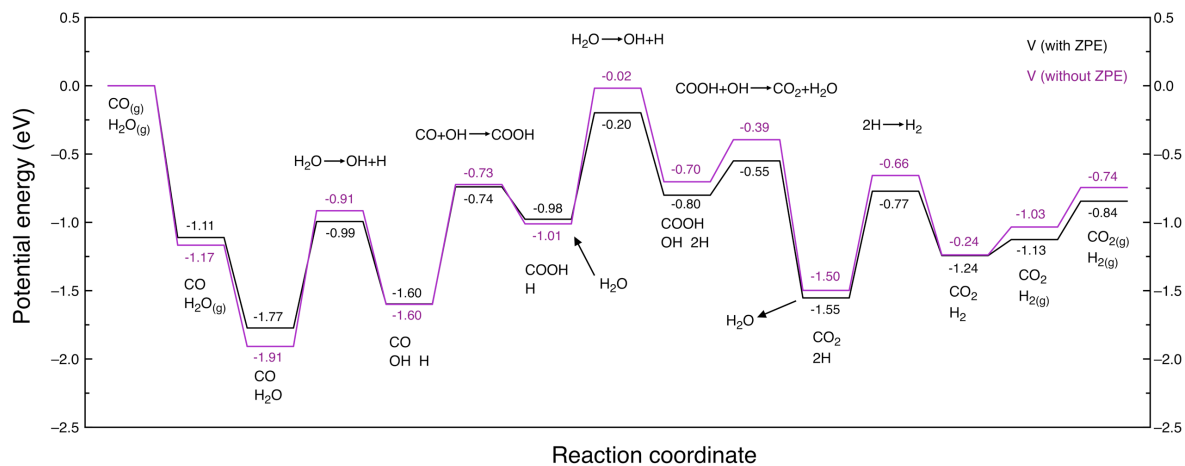


Figure 2. Simplified PEDs for the associative mechanism of the WGSR on Cu(321) with (blue) and without (red) the ZPE correction. The energy barriers are calculated for reactant species at infinite separation.

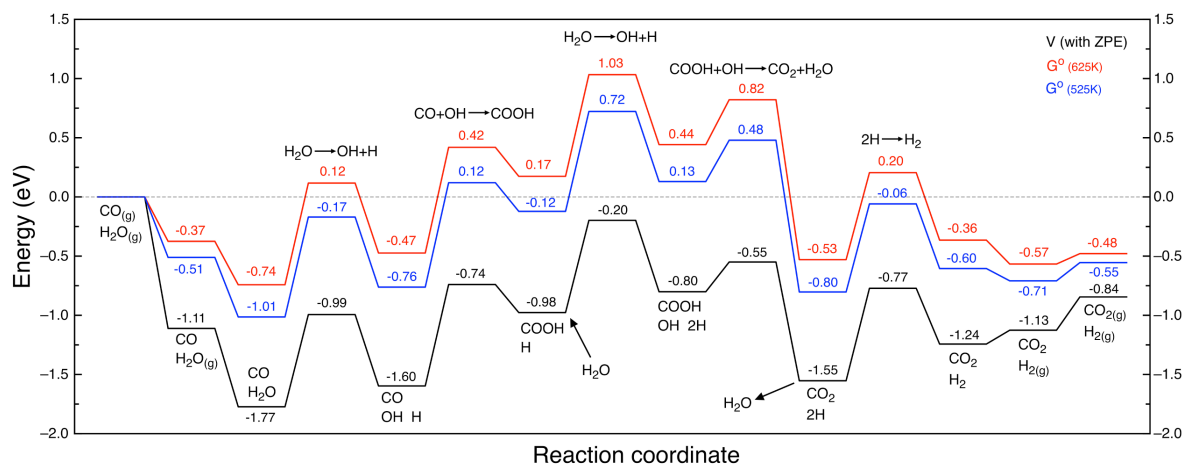


Figure 3. Comparison between PED with ZPE(black) and two Gibbs free energy diagrams ($P = 1$ bar, $T = 525$ K, blue and $T = 625$ K, red) for the associative mechanism of the WGS on Cu(321) surface (adsorbates at infinite separation).

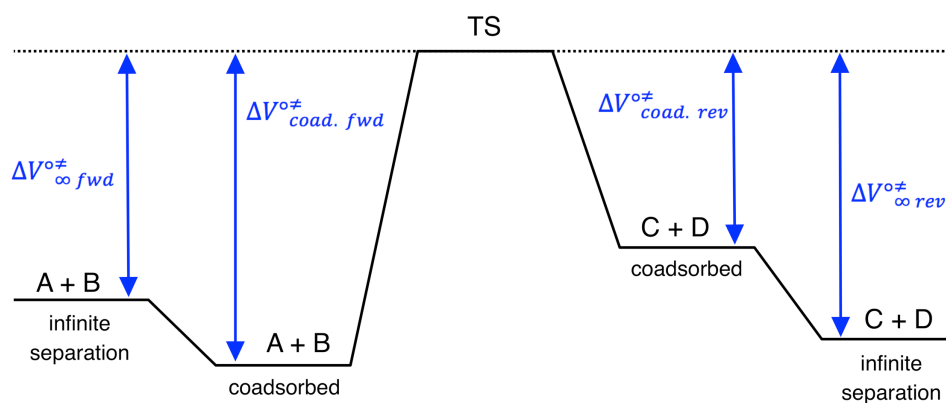


Figure 4. Potential energy profile for a bimolecular surface reaction $A + B \rightarrow C + D$ at zero-coverage limit.

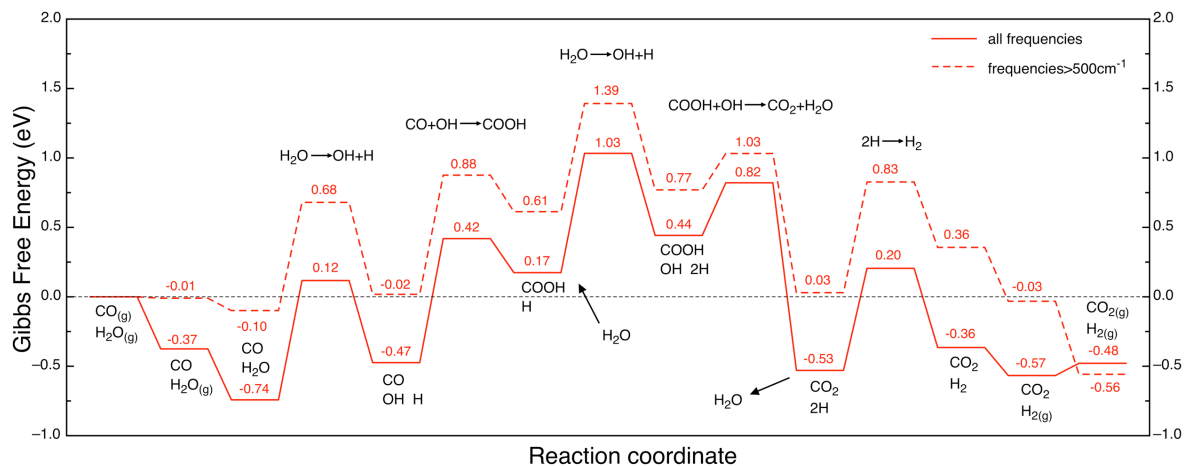


Figure 5. Gibbs free energy diagrams for the associative mechanism of the WGS on Cu(321) ($P = 1$ bar, $T = 625$ K). The correct profile computed using all the vibrational frequencies is plotted in solid line, whereas the same profile neglecting the frequencies below 500 cm^{-1} is plotted in dashed line.

Surface process	$ \Delta V^{0\ddagger} - \Delta G^{0\ddagger} $ (eV)		Q^\ddagger/Q_R	
	Forward	Reverse	Forward	Reverse
$\text{H}_2\text{O} \rightarrow \text{OH}+\text{H}$	0.08	0.01	0.22	1.26
$2\text{OH} \rightarrow \text{H}_2\text{O}+\text{H}$	0.06	0.09	0.34	0.18
$\text{CO}+\text{O} \rightarrow \text{CO}_2$	0.09	0.28	0.17	< 0.01
$\text{CO}+\text{OH} \rightarrow \text{COOH}$	0.04	0.01	0.51	0.87
$\text{COOH}+\text{OH} \rightarrow \text{CO}_2+\text{H}_2\text{O}$	0.13	0.35	0.09	< 0.01
$\text{H}+\text{H} \rightarrow \text{H}_2$	0.05	0.10	2.33	0.16

Table 1. Values of $|\Delta V^{0\ddagger} - \Delta G^{0\ddagger}|$ (eV) and Q^\ddagger/Q_R for different elementary surface processes of the WGSR on Cu(321) at 625 K.

T (K)	ΔG°	ΔG°	K_{eq}	K_{eq}
	525K	625K	525K	625K
PBE	-0.48	-0.41	41627	1905
PW91	-0.48	-0.41	43079	2046
B3LYP	-0.40	-0.36	7561	877
CCSD(T)	-0.12	-0.07	13	4
exp. ^[32]	-0.20	-0.16	80	20

Table 2. Comparison between experimental data and calculated values of the equilibrium constant (K_{eq}) and ΔG° of the overall WGSR, using an aug-cc-pVTZ basis set with different DFT functionals and the post-HF CCSD(T) method.

	TOF	coverage			
	(molec.·s ⁻¹ ·site ⁻¹)	CO	H ₂ O	OH	H
Diffusion	7826	2.7·10 ⁻⁴	1.2·10 ⁻²	1.8·10 ⁻¹	1.3·10 ⁻¹
No diffusion	6391	2.3·10 ⁻⁴	1.1·10 ⁻²	2.7·10 ⁻¹	1.6·10 ⁻¹

Table 3. Calculated turnover frequency and coverages of several adsorbates for the WGS on Cu(111) with and without including diffusion processes. kMC simulation conditions: T = 625 K, P_{CO} = 26 Torr and P_{H₂O} = 10 Torr.

	TOF (molec.·s ⁻¹ ·site ⁻¹)	coverage			
		CO	H ₂ O	OH	H
Lateral int.	199	1.3·10 ⁻¹	7.3·10 ⁻²	2.1·10 ⁻¹	3.6·10 ⁻²
No lateral int.	130	1.6·10 ⁻¹	5.1·10 ⁻²	2.8·10 ⁻¹	4.9·10 ⁻²

Table 4. Calculated turnover frequencies and coverages of several adsorbates for the WGS on Cu(321) with and without including lateral interactions in kMC simulations for T = 625 K, P_{CO} = 26 Torr and P_{H₂O} = 10 Torr.

References

- [1] J. K. Nørskov, F. Studt, F. Abild-Pedersen, T. Bligaard, *Fundamental Concepts in Heterogeneous Catalysis*, John Wiley & Sons, Inc., **2014**.
- [2] V. P. Zhdanov, *Surf. Sci.* **2002** *500*, 966.
- [3] K. J. Laidler, *Chemical Kinetics*, Harper & Row Publishers, New York, **1987**.
- [4] A.P.J. Jansen, *An introduction to kinetic Monte Carlo simulations of surface reactions*, Lecture Notes in Physics, vol. 856, Springer-Verlag, Heidelberg, **2012**.
- [5] K. Reuter, in: *Modeling and simulation of heterogeneous catalytic reactions*, (Ed: O. Deutschmann), Wiley-VCH Verlag GmbH and Co. KGaA, Weinheim, Germany, **2011**, p. 71-111.
- [6] M. Andersen, C. P. Plaisance, K. Reuter, *J. Chem. Phys.* **2017**, *147*, 152705.
- [7] A. Chatterjee, A.F. Voter, *J. Chem. Phys.* **2010**, *132*, 194101.
- [8] E. C. Dybeck, C.P. Plaisance, M. Neurock, *J. Chem. Theor. Comput.* **2017**, *13*, 1525.
- [9] L. Yang, A. Karim, J.T. Muckerman, *J. Phys. Chem. C* **2013**, *117*, 3414.
- [10] H. Prats, L. Álvarez, F. Illas, R. Sayós, *J. Catal.* **2016**, *333*, 217.
- [11] D. A. McQuarrie, *Statistical Mechanics*, Harper & Row, New York, **2000**.
- [12] L. Grabow, W. Schneider, M. J. Janik, T. Manz, A. van Duin, S. Sinnott, D. Scholl, *Computational Catalysis*, Royal Society of Chemistry Books, **2013**.
- [13] L. Kunz, F.M. Kuhn, O. Deutschmann, *J. Chem. Phys.* **2015**, *143*, 044108.
- [14] R. van de Vijver, N. M. Vandewiele, P. L. Bhoorasingh, B. L. Slakman, F. Seyedzadeh Khanshan, H.H. Carstensen, M.F. Reyniers, G. B. Marin, R. H. West, K.M. van Geem, *Int. J. Chem. Kinet.* **2015**, *47*, 199.
- [15] V. Morón, P. Gamallo, R. Sayós, *Theor. Chem. Acc.* **2011**, *128*, 683.
- [16] M. Van den Bossche, H. Grönbeck, *J. Am. Chem. Soc.* **2015**, *137*, 12035.
- [17] C. Callaghan, I. Fishtik, R. Datta, M. Carpenter, M. Chmielewski, A. Lugo, *Surf. Sci.* **2003**, *541*, 21.
- [18] N.A. Koryabkina, A.A. Phatak, W.F. Ruettinger, R.J. Farrauto, F.H. Ribeiro, *J. Catal.* **2003**, *217*, 233.
- [19] C.V. Ovesen, B.S. Clausen, B.S. Hammershøi, G. Steffensen, T. Askgaard, I. Chorkendorff, J.K. Nørskov, P.B. Rasmussen, P. Stoltze, P. Taylor, *J. Cat.* **1996**, *158*, 170.

-
- [20] C. J. Heard, C. Hu, M. Skoglundh, D. Creaser, H. Grönbeck, *ACS Catal.* **2016**, *6*, 3277.
- [21] H. Prats, P. Gamallo, F. Illas, R. Sayós, *J. Catal.* **2016**, *342*, 75.
- [22] J. Nielsen, M. d’Avezac, J. Hetherington, M. Stamatakis, *J. Chem. Phys.* **2013**, *139*, 224706.
- [23] M. Stamatakis, D.G. Vlachos, *ACS Catal.* **2012**, *2*, 2648.
- [24] M. Stamatakis, D.G. Vlachos, *J. Chem. Phys.* **2011**, *134*, 214115.
- [25] P.G. Moses, J.J. Mortensen, B.I. Lundqvist, J.K. Nørskov, *J. Chem. Phys.* **2009**, *130*, 104709.
- [26] P. Janthon, F. Viñes, S. M. Kozlov, J. Limtrakul, F. Illas, *J. Chem. Phys.* **2013**, *138*, 244701. [L]
[SEP]
- [27] B. A. De Moor, M. F. Reyniers, M. Sierka, J. Sauer, G. B. Marin, *J. Phys. Chem. C* **2008**, *112*, 11796. [L]
[SEP]
- [28] H. Prats, P. Gamallo, R. Sayós, F. Illas, *Phys. Chem. Chem. Phys.* **2016**, *18*, 2792.
- [29] J. Hermann, R.A. DiStasio Jr., A. Tkatchenko, *Chem. Rev.* **2017**, *117*, 4714.
- [30] K. Reuter, M. Scheffler, *Phys. Rev. B* **2006**, *73*, 045433.
- [31] S. Chakrabarty, T. Das, P. Banerjee, R. Thapa, G.P. Das, *Appl. Surf. Sci.* **2017**, *418*, 92.
- [32] D. Mendes, A. Mendes, L.M. Madeira, A. Iulianelli, J.M. Sousa, A. Basile, *Asia-Pac. J. Chem. Eng.* **2010**, *5*, 111.
- [33] Gaussian 09, Revision D.01, M.J. Frisch, G.W. Trucks, H.B. Schlegel, G.E. Scuseria, M.A. Robb, J.R. Cheeseman, G. Scalmani, V. Barone, B. Mennucci, G.A. Petersson, H. Nakatsuji, M. Caricato, X. Li, H.P. Hratchian, A.F. Izmaylov, J. Bloino, G. Zheng, J.L. Sonnenberg, M. Hada, M. Ehara, K. Toyota, R. Fukuda, J. Hasegawa, M. Ishida, T. Nakajima, Y. Honda, O. Kitao, H. Nakai, T. Vreven, J.A. Montgomery Jr., J.E. Peralta, F. Ogliaro, M. Bearpark, J.J. Heyd, E. Brothers, K.N. Kudin, V.N. Staroverov, R. Kobayashi, J. Normand, K. Raghavachari, A. Rendell, J. C. Burant, S.S. Iyengar, J. Tomasi, M. Cossi, N. Rega, J.M. Millam, M. Klene, J.E. Knox, J.B. Cross, V. Bakken, C. Adamo, J. Jaramillo, R. Gomperts, R.E. Stratmann, O. Yazyev, A.J. Austin, R. Cammi, C. Pomelli, J.W. Ochterski, R.L. Martin, K. Morokuma, V.G. Zakrzewski, G.A. Voth, P.

Salvador, J.J. Dannenberg, S. Dapprich, A.D. Daniels, Ö. Farkas, J.B. Foresman, J.V. Ortiz, J. Cioslowski, D.J. Fox, Gaussian Inc, Wallingford, CT, **2013**.

[34] A. D. Becke, *J. Chem. Phys.* **1993**, *98*, 5648.

[35] S. F. Sousa, P.A. Fernandes, M.J. Ramos, *J. Phys. Chem. A* **2007**, *111*, 10439.

[36] P. Janthon, S. Luo, S.M. Kozlov, F. Viñes, J. Limtrakul, D.G. Truhlar, F. Illas, *J. Chem. Theory Comput.* **2014**, *10*, 3832.

[37] P. Janthon, S.M. Kozlov, F. Viñes, J. Limtrakul, F. Illas, *J. Chem. Theory Comput.* **2013**, *9*, 1631.

[38] A. Notario-Estévez, S.M. Kozlov, F. Viñes, F. Illas, *Chem. Commun.* **2015**, *51*, 5602.

[39] Y. Zhao, D.G. Truhlar, *J. Chem. Phys.* **2006**, *124*, 224105.

[40] N.E. Schultz, Y. Zhao, D.G. Truhlar, *J. Phys. Chem. A* **2005**, *109*, 11127.

[41] J. Paier, M. Marsman, G. Kresse, *J. Chem. Phys.* **2007**, *127*, 024103.

[42] J.L.C. Fajín, M.N.D.S. Cordeiro, J.R.B. Gomes, F. Illas, *J. Chem. Theory Comput.* **2012**, *8*, 1737. ^[1] _[SEP]

[43] L. Thian, C. Huo, D. Cao, Y. Yang, J. Xu, B. Wu, H. Xiang, Y. Xu, Y. Li, *J. Molec. Struct. THEOCHEM* **2010**, *941*, 30.

[44] S. Piccinin, M. Stamatakis, *ACS Catal.* **2014**, *4*, 2143.

[45] M.J. Hoffmann, K. Reuter, *Top. Catal.* **2014**, *57*, 159.

[46] E. Vignola, S.N. Steinmann, B.D. Vandegehuchte, D. Curulla, M. Stamatakis, P. Sautet, *J. Chem. Phys.* **2017**, *147*, 054106.

[47] R.B. Getman, W.F. Schneider, *Chem. Cat. Chem.* **2010**, *2*, 1450.

[48] J.K. Nørskov, T. Bligaard, A. Logadottir, S. Bahn, L.B. Hansen, M. Bollinger, H. Bengaard, B. Hammer, Z. Sljivancanin, M. Mavrikakis, Y. Xu, S. Dahl, J.H. Jacobsen, *J. Catal.* **2002**, *209*, 275.

[49] P. Gamallo, M. González, R. Sayós, *J. Chem. Phys.* **2003**, *119*, 2545.

[50] A.A. Gokhale, J.A. Dumestic, M. Mavrikakis, *J. Am. Chem. Soc.* **2008**, *130*, 1402.

[51] J.L.C. Fajín, M.N.D.S. Codeiro, F. Illas, J.R.B. Gomes, *J. Catal.* **2009**, *268*, 131.

[52] L.C. Grabow, A.A. Gokhale, S.T. Evans, J.A. Dumesic, M. Mavrikakis, *J. Phys. Chem. C* **2008**, *112*, 4608.

[53] G. Wang, L. Jiang, Z. Cai, Y. Pan, X. Zhao, W. Huang, K. Xie, Y. Li, Y. Sun, B. Zhong, *J. Phys. Chem. B* **2003**, *107*, 557.

-
- [54] Y.C. Huang, T. Zhou, C. Ling, S. Wang, J.Y. Du, *ChemPhysChem* **2014**, *15*, 2490.
- [55] S.-C. Huang, C.-H. Lin, J.-H. Wang, *J. Phys. Chem. C* **2010**, *114*, 9826.
- [56] C.T. Campbell, *Top. Catal.* **1994**, *1*, 353.
- [57] C.T. Campbell, *ACS Catal.* **2017**, *7*, 2770.